Published by Nigerian Society of Physical Sciences. Hosted by FLAYOO Publishing House LTD

Proceedings of the Nigerian Society of Physical Sciences

Journal Homepage: https://flayoophl.com/journals/index.php/pnspsc

Modelling the effect of vaccination on the dynamics of tuberculosis in an age-structured population

Omowumi Fatimah Lawal[a,*], Afeez Abidemi[b]

[a]*Department of Mathematical Sciences, Bamidele Olumilua University of Education, Science, and Technology, Ikere-Ekiti, P.M.B. 250, Ekiti State, Nigeria*
[b]*Department of Mathematical Sciences, Federal University of Technology Akure, P.M.B. 704, Ondo State, Nigeria*

A B S T R A C T

Despite several efforts, Tuberculosis (TB) is still a global leading cause of death. This paper proposed an age-structured deterministic model governing the transmission dynamics and control of TB in the presence of vaccination integrated into the eligible population. Qualitative analysis of the model was carried out to obtain the disease-free equilibrium point of it. The effective reproduction number, $\mathcal{R}_e$, of the model was calculated using the next generation matrix method, which offered a numerical indicator of the potential for TB transmission in the age-structured population. Numerical analysis further offers some insightful information about how the key sensitive parameters and the vaccination rate influence the transmission dynamics and control of TB in an age-structured population settings.

Keywords: Tuberculosis, Age-structured population, Effective reproduction number, Vaccination.

DOI:10.61298/pnspsc.2025.2.179

1. INTRODUCTION

Tuberculosis (TB) is an infectious disease that most frequently affects the lungs, but it can also affect the brain, lymph nodes,kidneys, bones, joints, ear, urinary tract, spine, skin and other parts of the body [1, 2]. TB is caused by a type of bacteria called *Mycobacterium tuberculosis* (Mtb) [3].

It spreads through the air when infected people cough, sneeze or spit [3, 4]. A few germs inhaled by an individual can cause TB infection. Most of the infected individuals with Mtb are capable to control the infection and remain in a latent stage in which they cannot transmit the disease [4].

It is believed that approximately 25% of the world population has contracted TB bacteria; however, the majority of those infected will not develop TB disease, and some will recover from the infection [3].

Despite significant advancements in prevention and treatment, tuberculosis disease continues to be the global leading cause of death, the leading cause of death for individuals living with HIV, and a major contributor to antimicrobial resistance [1, 2].

Interestingly, about one-fourth of the world population is infected with Mtb, with approximately 10 million cases and 1.5 million deaths annually [1, 3]. It is however, treatable if an early diagnosis is made and the right treatment plan is followed, which may take six months to two years for active TB to clear [1]. In addition to posing a major health concern to low and middle in-

*Corresponding Author Tel. No.: +234-803-5202-740.
e-mail: lawal.fatimah@bouesti.edu.ng (Omowumi Fatimah Lawal)

come countries, TB affects economic growth negatively [1].

A host of mathematical modelling work on infectious diseases like typhoid fever, Dengue Fever, COVID-19, yellow fever, TB, cholera, malaria, HIV, among others, have been done [5–11]. In addition, many modelling works on TB have been carried out, for instance, Ronoh *et al.* [1] extends the standard SEIRS epidemiology model of TB to include MDR-TB, focusing on susceptible, exposed, infected, resistant, and recovered humans. The basic reproduction number was calculated, and the existence of disease-free equilibrium and endemic equilibrium was confirmed. Numerical analysis showed that both active and MDR-TB strains persist due to a lack of permanent immunity, while recovered individuals can lose immunity and become susceptible again.

Also, Hogan *et al.* [12] use mathematical modelling approach in understanding transmissible infections' dynamics. The authors used a common childhood infection as a case study and examined age structures in compartmental differential equation models. The research shows that incorporating age structures does not alter the overall dynamics, but it is helpful in simulating age-dependent intervention strategies.

Similarly, Peter *et al.* [13] presented a deterministic model for the population dynamics of Mtb, the causative agent of TB, focusing on the impact of competition among bacteria on infection prevalence. Mtb population was assumed to have two types of growth. The model qualitative analysis and numerical results suggest forward, backward, and S-shaped bifurcations when the reproduction number is less than unity and up to three bacteria-present equilibria namely, two locally asymptotically stable, and one unstable.

Sangotola *et al.* [14] developed a five-compartment model to comprehend the dynamics of TB in communities. When the basic reproduction number is less than one, it shows a locally asymptotically stable disease-free equilibrium point; when it is above one, it reveals an endemic equilibrium. Control measures were evaluated using numerical simulations and sensitivity analysis. Their research suggests the optimal ways to control TB, emphasizing early treatment and prevention strategies,which were both effective.

In Moya *et al.* [15], a mathematical model was developed to study the effectiveness of therapy in TB, and the impact of HIV/AIDS and diabetes on TB spread and drug resistance. The model considered the relationship among TB, HIV/AIDS and diabetes, as well as the behavior of multi-drug resistance (MDR-TB) and extensively drug-resistant (XDR-TB). Analysis of the model showed that MDR-TB and XDR-TB halt TB control, with a more significant number of drug-sensitive TB cases in infected compartments. The study suggests increasing attention to the diabetic population, improving glucose control, and raising specialized medical consultations to achieve permanence in TB treatment and control the entry of individuals to the diabetic compartments by diabetes tests.

However, studies on the use of age-structured deterministic model to assess the transmission dynamics and control of TB are limited in the literature. Thus, this study proposes an age-structured compartmental model that divides the entire population into two: the vaccine target population and the non-vaccine target population. Consequently, this study aims to examine the impact of vaccination integrated into the eligible population on the spread and control of TB.

Table 1. Description of the model's variables.

Variable	Description
N	Total human population
S_1	Population of vaccine-target susceptible individuals
E_1	Population of vaccine-target exposed individuals
I_1	Population of vaccine-target symptomatic infectious individuals
C_1	Population of vaccine-target carrier individuals
T_1	Population of vaccine-target treated individuals
R_1	Population of vaccine-target recovered individuals
V_1	Population of vaccinated individuals
S_2	Population of non-vaccine-target susceptible individuals
E_2	Population of non-vaccine target exposed individuals
I_2	Population of non-vaccine target symptomatic infectious individuals
C_2	Population of non-vaccine target carrier individuals
T_2	Population of non-vaccine target treated individuals
R_2	Population of non-vaccine target recovered individuals
V_2	Population of vaccinated individuals in the non-vaccine target age group

The remaining parts of the article are structured as follows: Section 2 discusses the formulation of the model. In Section 3, the positivity and boundedness of the model solution, and detailed qualitative analysis of the model are carried out. In section 4, simulations of the model is conducted, the results are presented and discussed, while in Section 5, concluding remarks from the study are given. This section also highlights the direction for further studies.

2. MODEL FORMULATION

In this section, we propose a deterministic model describing the transmission dynamics and control of TB in an age-structured setting. The total population under consideration is split into two age group of 6 months to 45 years and 46 years and above. Individuals in the age class 6 months to 45 years are considered to be vaccine-eligible (vaccine-target) population, while individuals in the age class 45 years and above are assumed to be non-vaccine-eligible (non-vaccine-target) population. Each of the age-group population is further divided into seven non-intersecting compartments of susceptible individuals, S, exposed individuals, E, symptomatic infectious individuals, I, carriers, C, treated individuals, T, recovered individuals, R, and vaccinated individuals, V. Using the indices 1 and 2 to denote the compartments related to the age-group 1 and 2, respectively, the total population at any time t, denoted by $N(t)$, is mathematically represented as

$$\begin{aligned} N(t) = {} & S_1(t) + E_1(t) + I_1(t) + C_1(t) + T_1(t) \\ & + R_1(t) + V_1(t) + S_2(t) + E_2(t) + I_2(t) \\ & + C_2(t) + T_2(t) + R_2(t) + V_2(t). \end{aligned} \tag{1}$$

Consequently, the age-structured deterministic compartmental model governing the dynamics of TB transmission and control is a system of ordinary differential equations given by

$$\begin{aligned} \frac{dS_1}{dt} &= \Lambda + \xi V_1 - \beta_1 \frac{(C_1 + \sigma_1 I_1 + C_2 + \sigma_2 I_2)S_1}{N} \\ &\quad - (\theta + \mu + \epsilon)S_1 + \omega R_1, \\ \frac{dE_1}{dt} &= \beta_1 \frac{(C_1 + \sigma_1 I_1 + C_2 + \sigma_2 I_2)S_1}{N} - (\gamma + \mu + \epsilon)E_1, \end{aligned}$$

Table 2. Description of the model's parameters.

Parameter	Description
Λ	Recruitment rate for human population
μ	Human natural death rate
ϕ_1	Rate of carrier progressing to symptomatic infectious in vaccine-target age group
ϕ_2	Progression rate from carrier to symptomatic infectious in non-vaccine target age group
ϵ	Maturation rate
β_1	Effective transmission rate of TB from carriers and symptomatic individuals to the susceptible individuals in the vaccine-target age group
β_2	Effective transmission rate of TB from carriers and symptomatic individuals to the susceptible individuals in the non-vaccine target age group
η	Mass testing and treatment rate for carriers
γ	Progression rate from exposed to infectious classes (symptomatic and carrier)
σ_1	Reduction parameter for the transmission rate of TB from symptomatic individuals in the age group 1 to susceptible individuals in the vaccine-target age group relative to the transmission by carriers
σ_2	Reduction parameter for the transmission rate of TB from symptomatic individuals in the age group 2 to susceptible individuals in the vaccine-target age group relative to the transmission by carriers
σ_3	Reduction parameter for the transmission rate of TB from symptomatic individuals in the age group 1 to susceptible individuals in the non-vaccine-target age group relative to the transmission by carriers
σ_4	Reduction parameter for the transmission rate of TB from symptomatic individuals in the age group 2 to susceptible individuals in the non-vaccine-target age group relative to the transmission by carriers
ξ	Vaccine waning rate
δ_1	TB-induced death rate in symptomatic infectious people
δ_2	Disease-induced death in treated individuals
ω	Natural immunity loss
κ	Proportion of exposed human that becomes symptomatic
θ	The vaccination rate for vaccine-eligible age group
τ	Treatment rate for symptomatic infectious individuals in age group 1
r_1	Recovery rate for treated individuals
r_2	Natural recovery rate for carriers

$$
\begin{aligned}
\frac{dI_1}{dt} &= \kappa\gamma E_1 - (\tau + \delta_1 + \mu + \epsilon)I_1 + \phi_1 C_1,\\
\frac{dC_1}{dt} &= (1-\kappa)\gamma E_1 - (\phi_1 + \mu + \eta + r_2 + \epsilon)C_1,\\
\frac{dT_1}{dt} &= \tau I_1 + \eta C_1 - (\delta_2 + r_1 + \mu + \epsilon)T_1,\\
\frac{dR_1}{dt} &= r_2 C_1 + r_1 T_1 - (\mu + \omega + \epsilon)R_1,\\
\frac{dV_1}{dt} &= \theta S_1 - (\mu + \xi + \epsilon)V_1,\\
\frac{dS_2}{dt} &= \epsilon S_1 - \beta_2 \frac{(C_1 + \sigma_3 I_1 + C_2 + \sigma_4 I_2)S_2}{N}\\
&\quad - \mu S_2 + \xi V_2 + \omega R_2,\\
\frac{dE_2}{dt} &= \epsilon E_1 + \beta_2 \frac{(C_1 + \sigma_3 I_1 + C_2 + \sigma_4 I_2)S_2}{N} - (\gamma + \mu)E_2,\\
\frac{dI_2}{dt} &= \kappa\gamma E_2 - (\tau + \delta_1 + \mu)I_2 + \epsilon I_1 + \phi_2 C_2,\\
\frac{dC_2}{dt} &= (1-\kappa)\gamma E_2 - (\phi_2 + \mu + \eta + r_2)C_2 + \epsilon C_1,\\
\frac{dT_2}{dt} &= \tau I_2 + \eta C_2 - (\delta_2 + r_1 + \mu)T_2 + \epsilon T_1,\\
\frac{dR_2}{dt} &= r_2 C_2 + r_1 T_2 - (\mu + \omega)R_2 + \epsilon R_1,\\
\frac{dV_2}{dt} &= \epsilon V_1 - (\xi + \mu)V_2,
\end{aligned} \tag{2}
$$

with the initial conditions at time $t = 0$ given by:

$$
\begin{aligned}
&S_1(0) > 0,\ E_1(0) \geq 0,\ I_1(0) > 0,\ C_1(0) \geq 0,\ T_1(0) \geq 0,\\
&R_1(0) \geq 0, V_1(0) \geq 0, S_2(0) > 0, E_2(0) \geq 0, I_2(0) > 0,\\
&C_2(0) \geq 0,\ T_2(0) \geq 0,\ R_2(0) \geq 0,\ V_2(0) \geq 0.
\end{aligned} \tag{3}
$$

In Table 1, the state variables of model (2) are further described, while Table 2 gives the physical meaning of each of the parameters of the model.

3. MODEL ANALYSIS

3.1. POSITIVITY OF SOLUTIONS

It is known that all the model parameters in Table 2 are positive. Thus, it is important to show that none of the state variables of the model can ever be negative. Hence, from the first differential equation of the model (2):

$$
\begin{aligned}
\frac{dS_1}{dt} &= \Lambda + \xi V_1 + \omega R - \beta_1 \frac{(C_1 + \sigma_1 I_1 + C_2 + \sigma_2 I_2)S_1}{N}\\
&\quad - (\theta + \mu + \epsilon)S_1\\
&\geq -\left[\beta_1 \frac{(C_1 + \sigma_1 I_1 + C_2 + \sigma_2 I_2)S_1}{N} + (\theta + \mu + \epsilon)S_1(t)\right],\\
\frac{dS_2}{dt} &= \epsilon S_1 + \xi V_2 - \beta_2 \frac{(C_1 + \sigma_3 I_1 + C_2 + \sigma_4 I_2)S_2}{N} - \mu S_2\\
&\geq -[\beta_2 \frac{(C_1 + \sigma_3 I_1 + C_2 + \sigma_4 I_2)S_2}{N} + \mu S_2(t)],
\end{aligned} \tag{4}
$$

for all $t \geq 0$ since $S_1(t) \geq 0$ and $S_2(t) \geq 0$ for all $t \geq 0$. Using integrating factor method, Equation (4) yields:

$$S_1(t) \geq S_1(0) \exp\left(-\left[m_1 t + \int_0^t \frac{\beta_1(C_1 + \sigma_1 I_1 + C_2 + \sigma_2 I_2)S_1}{N} d\tau\right]\right), \tag{5}$$

where $m_1 = \theta + \mu + \epsilon$ and

$$S_2(t) \geq S_2(0) \exp\left(-\left[\mu t + \int_0^t \frac{\beta_2(C_1 + \sigma_2 I_1 + C_2 + \sigma_4 I_2)S_2}{N} d\tau\right]\right),$$

for all $t \geq 0$. Following the same routine, it is easy to derive the following inequalities for the other state variables:

$$\begin{aligned}
E_1(t) &\geq E_1(0) \exp\left(-(\gamma + \mu + \epsilon)t\right), \forall t \geq 0,\\
I_1(t) &\geq I_1(0) \exp\left(-(\tau + \delta_1 + \mu + \epsilon)t\right), \forall t \geq 0,\\
C_1(t) &\geq C_1(0) \exp\left(-(\phi_1 + \mu + \delta_2 + \eta + r_2 + \epsilon)t\right), \forall t \geq 0\\
T_1(t) &\geq T_1(0) \exp\left(-(\delta_2 + r_1 + \mu + \epsilon)t\right), \forall t \geq 0,\\
R_1(t) &\geq R_1(0) \exp\left(-(\mu + \omega + \epsilon)t\right), \forall t \geq 0,\\
V_1(t) &\geq V_1(0) \exp\left(-(\mu + \xi + \epsilon)\right), \forall t \geq 0,\\
E_2(t) &\geq E_2(0) \exp\left(-(\gamma + \mu)t\right), \forall t \geq 0,\\
I_2(t) &\geq I_2(0) \exp\left(-(\tau + \delta_1 + \mu)t\right), \forall t \geq 0,\\
C_2(t) &\geq C_2(0) \exp\left(-(\phi_2 + \mu + \delta_2 + \eta + r_2)t\right), \forall t \geq 0,\\
T_2(t) &\geq T_2(0) \exp\left(-(\delta_2 + r_1 + \mu)t\right), \forall t \geq 0,\\
R_2(t) &\geq R_2(0) \exp\left(-(\mu + \omega)t\right), \forall t \geq 0,\\
V_2(t) &\geq V_2(0) \exp\left(-(\mu + \xi)\right), \forall t \geq 0.
\end{aligned}$$

From the above analysis, the following result is established:

Theorem 3.1. *All the state variables $S_1(t)$, $E_1(t)$, $I_1(t)$, $C_1(t)$, $T_1(t)$, $R_1(t)$, $V_1(t)$, $S_2(t)$, $E_2(t)$, $I_2(t)$, $C_2(t)$, $T_2(t)$, $R_2(t)$,and $S_2(t)$ of the TB model (2) with positive initial conditions $S_1(0) > 0$, $E_1(0) \geq 0$, $I_1(0) > 0$, $C_1(0) \geq 0$, $T_1(0) \geq 0$, $R_1(0) \geq 0$, $V_1(0) \geq 0$, $S_2(0) \geq 0$, $E_2(0) \geq 0$, $I_2(0) > 0$, $C_2(0) \geq 0$, $T_2(0) \geq 0$, $R_2(0) \geq 0$ and $V_2(0) \geq 0$ remain positive for all time $t \geq 0$.*

Hence, the feasible region for the TB model (2) is defined by $\Pi \subset \mathbb{R}_+^{14}$, where

$$\begin{aligned}
\Pi = \{&(S_1(t), E_1(t), I_1(t), C_1(t), T_1(t), R_1(t), V_1(t), S_2(t), E_2(t),\\
&I_2(t), C_2(t), T_2(t), R_2(t), V_2(t)) \in \mathbb{R}_+^{14} : N(t) \leq \frac{\Lambda}{\mu}\Big\}.
\end{aligned} \tag{6}$$

3.2. EXISTENCE OF DISEASE-FREE EQUILIBRIUM

The disease-free equilibrium (DFE) of model (2), denoted by Ψ, is the steady state solution of the model when there is no disease in the population. That is, when

$$\begin{aligned}
\frac{dS_1}{dt} = \frac{dE_1}{dt} = \frac{dI_1}{dt} = \frac{dC_1}{dt} = \frac{dT_1}{dt} = \frac{dR_1}{dt} = \frac{dV_1}{dt} = 0,\\
\frac{dS_2}{dt} = \frac{dE_2}{dt} = \frac{dI_2}{dt} = \frac{dC_2}{dt} = \frac{dT_2}{dt} = \frac{dR_2}{dt} = \frac{dV_2}{dt} = 0,
\end{aligned}$$

and $E_1 = I_1 = C_1 = T_1 = E_2 = I_2 = C_2 = T_2 = 0$. Consequently, the following sub-system of equations emerges from model (2):

$$\begin{aligned}
\Lambda + \xi V_1 - (\theta + \mu + \epsilon)S_1 &= 0,\\
\theta S_1 - (\mu + \xi + \epsilon)V_1 &= 0,\\
\epsilon S_1 - \mu S_2 + \xi V_2 &= 0,\\
\epsilon V_1 - (\xi + \mu)V_2 &= 0.
\end{aligned}$$

Table 3. Model parameter values.

Parameter	Baseline Value	Source
ω	0.05	[1]
β_1	0.6501	[13]
β_2	0.8501	Assumed
σ_1	0.9	Assumed
σ_2	0.8	Assumed
σ_3	0.9	Assumed
σ_4	0.8	Assumed
Λ	1364	[16]
θ	0.05	[16]
ξ	0.067	[13]
μ	0.43e-4*365	[16]
r_1	0.01	[13]
r_2	0.005	[13]
γ	0.00375	[13]
δ_1	0.00001	[1]
δ_2	0.00005	[13]
τ	0.01	[16]
ϵ	1/45	[2, 3]
κ	0.129	[17]
ϕ_1	0.075	[16]
ϕ_2	0.075	[16]
η	0.015	Assumed

Solving the above equations simultaneously, the DFE is obtained as:

$$\Psi = (S_1^*, E_1^*, I_1^*, C_1^*, T_1^*, R_1^*, V_1^*, S_2^*, E_2^*, I_2^*, C_2^*, T_2^*, R_2^*, V_2^*), \tag{7}$$

where the components of Ψ in (7) are given by

$$\begin{aligned}
S_1^* &= \frac{\Lambda m_7}{m_1 m_7 - \theta\xi},\\
V_1 &= \frac{\theta\Lambda m_7}{m_7(m_1 m_7 - \theta\xi)},\\
S_2 &= \frac{\epsilon m_7 \Lambda(m_7 m_{13} + \theta\xi)}{\mu m_7 m_{13}(m_1 m_7 - \theta\xi)},\\
V_2 &= \frac{(m_1 m_7 - \theta\xi)\epsilon\Lambda + \theta\Lambda\epsilon m_7 + \epsilon\xi\Lambda}{m_7 m_{13}(m_1 m_7 - \theta\xi)},
\end{aligned}$$

with $m_7 = \mu + \xi + \epsilon$ and $m_{13} = \mu + \xi$.

3.3. CONTROL REPRODUCTION NUMBER

Control reproduction number (denoted as $\mathcal{R}_e$), also known as effective reproduction number, is defined as the average number of secondary case per infectious case in a population made up of both susceptible and vaccinated hosts [18]. It helps to determine the level of preventive and control measures required to control an outbreak.

In this paper, the Next Generation Matrix method popularised by the authors in Ref. [19] is employed to compute the $\mathcal{R}_e$ of model (2). Let $x = (E_1, I_1, C_1, T_1, E_2, I_2, C_2, T_2)^T$ be the infected compartments in the TB model (2). Then, it can be deduced from the model that:

$$\frac{dx}{dt} = \mathcal{F}(x) - \mathcal{V}(x),$$

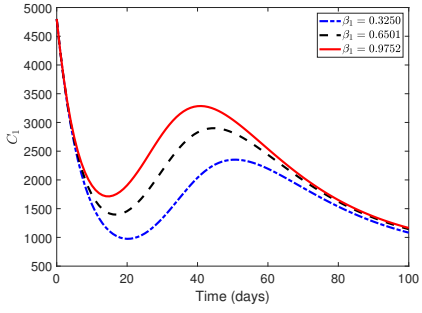

(a) Carriers in vaccine target population

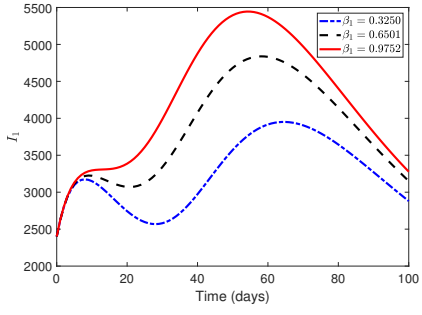

(b) Symptomatic Infectious in vaccine target population.

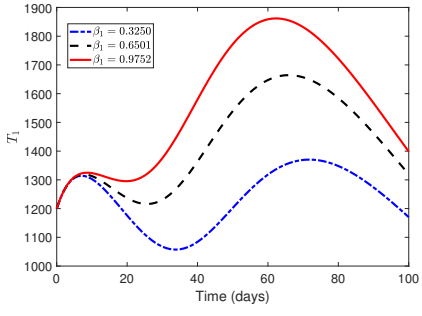

(c) Treated individuals in vaccine target population

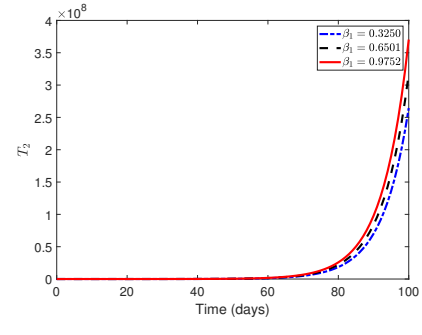

(d) Treated individuals in non-vaccine target population

Figure 1. Simulation displaying the dynamics of the states variables of model (2) with varying effective transmission rate of TB from carriers and symptomatic infectious individuals to vaccine target susceptible populations.

where

$$\mathcal{F} = \begin{pmatrix} \frac{\beta_1(\sigma_1 I_1 + \sigma_2 I_2 + C_1 + C_2)S_1}{N} \\ 0 \\ 0 \\ 0 \\ \frac{\beta_2(\sigma_3 I_1 + \sigma_4 I_2 + C_1 + C_2)S_2}{N} \\ 0 \\ 0 \\ 0 \end{pmatrix}, \tag{8}$$

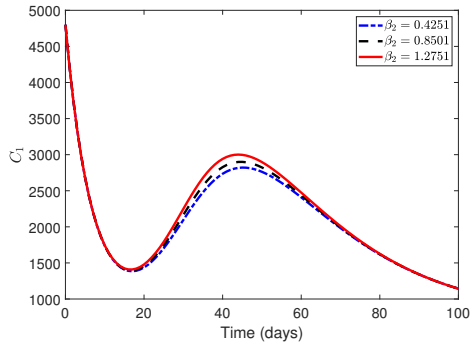

(a) Carriers

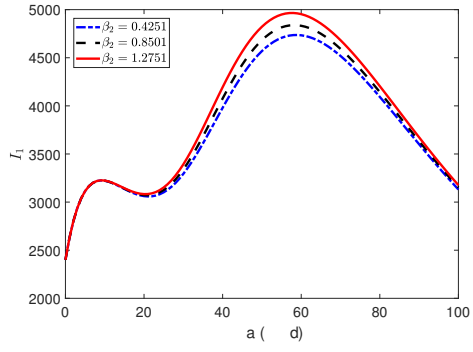

(b) Symptomatic Infectious

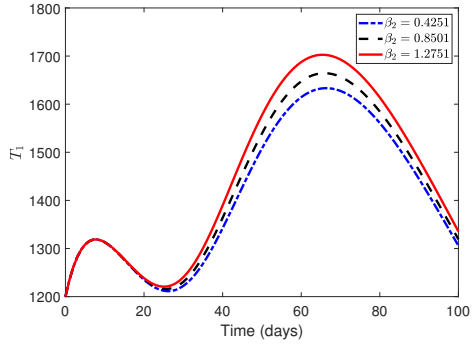

(c) Treated

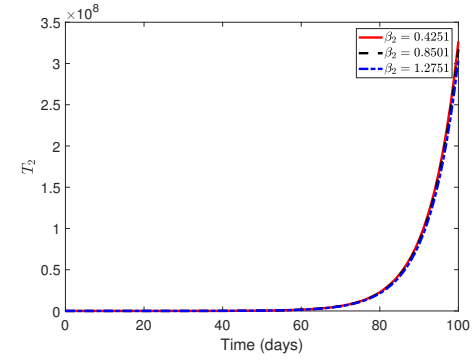

(d) Treated

Figure 2. Simulation demonstrating the dynamics of the states variables of model (2) with varying effective transmission rate of TB from carriers and symptomatic infectious individuals to non vaccine target susceptible populations.

and

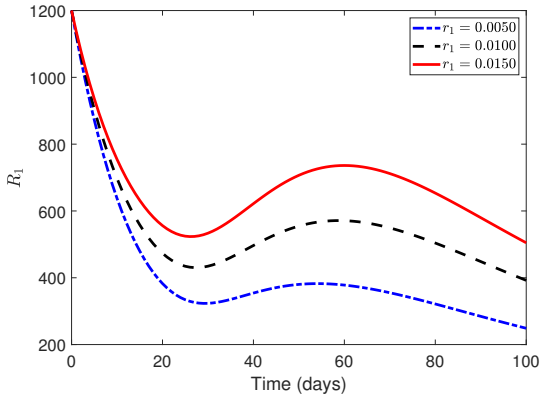

(a) Recovery due to treatment in vaccine target population.

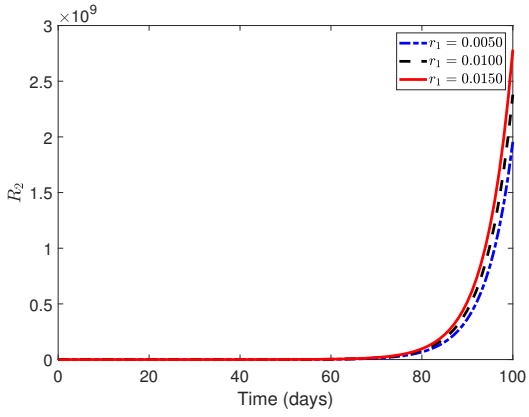

(b) Recovery due to treatment in non- vaccine target population.

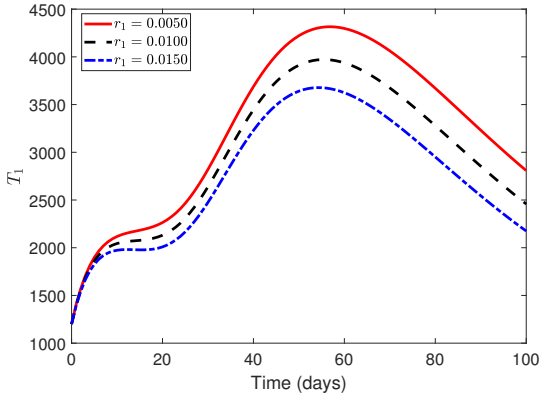

(c) Recovery of treated individual in vaccine target susceptible population.

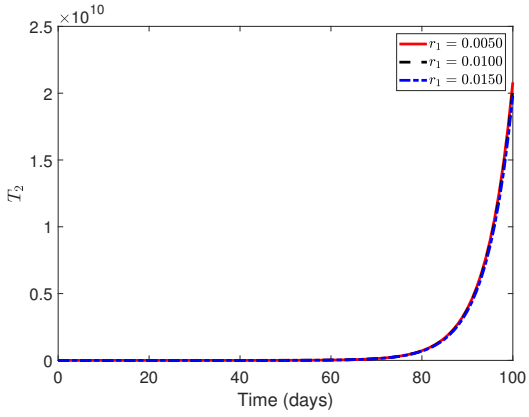

(d) Recovery of treated in non-vaccine target individuals.

Figure 3. Simulation showing the dynamics of the states variables of model (2) with varying recovery due to treatment of TB from carriers and symptomatic infectious.

$$\mathcal{V} = \begin{pmatrix} m_2 E_1 \\ -\gamma\kappa E_1 - C_1\phi_1 + m_3 I_1 \\ -\gamma(1-\kappa)E_1 + m_4 C_1 \\ -\eta C_1 - \tau I_1 + m_5 T_1 \\ -\epsilon E_1 + m_7 E_2 \\ -\gamma\kappa E_2 - \epsilon I_1 - C_2\phi_2 + m_8 I_2 \\ -\gamma(1-\kappa)E_2 - \epsilon C_1 + m_9 C_2 \\ -\epsilon T_1 - \eta C_2 - \tau T_2 + m_{10} T_2 \end{pmatrix}, \tag{9}$$

where

$$m_2 = \gamma + \mu + \epsilon, m_3 = \tau + \delta_1 + \mu + \epsilon,$$
$$m_4 = \phi_1 + \mu + \delta_2 + \eta + r_2 + \epsilon, m_5 = \delta_2 + r_1 + \mu + \epsilon,$$
$$m_6 = \mu + \omega + \epsilon, m_8 = \gamma + \mu, m_9 = \tau + \delta_1 + \mu,$$
$$m_{10} = \phi_2 + \mu + \delta_2 + \eta + r_2, m_{11} = \delta_2 + r_1 + \mu, m_{12} = \mu + \omega.$$

Thus, the matrix of the new infection terms $\mathcal{F}$ and matrix of the transition terms $\mathcal{V}$ are the corresponding Jacobian matrices evaluated at the DFE Ψ, and are derived as:

$$F = \begin{pmatrix} 0 & \frac{\beta_1\sigma_1 S_1^*}{N^*} & \frac{\beta_1 S_1^*}{N^*} & 0 & 0 & \frac{\beta_1\sigma_2 S_1^*}{N^*} & \frac{\beta_1 S_1^*}{N^*} & 0 \\ 0 & 0 & 0 & 0 & 0 & 0 & 0 & 0 \\ 0 & 0 & 0 & 0 & 0 & 0 & 0 & 0 \\ 0 & 0 & 0 & 0 & 0 & 0 & 0 & 0 \\ 0 & \frac{\beta_2\sigma_3 S_2^*}{N^*} & \frac{\beta_2 S_2^*}{N^*} & 0 & 0 & \frac{\beta_2\sigma_4 S_2^*}{N^*} & \frac{\beta_2 S_2^*}{N^*} & 0 \\ 0 & 0 & 0 & 0 & 0 & 0 & 0 & 0 \\ 0 & 0 & 0 & 0 & 0 & 0 & 0 & 0 \\ 0 & 0 & 0 & 0 & 0 & 0 & 0 & 0 \end{pmatrix}, \tag{10}$$

and

$$V = \begin{pmatrix} m_2 & 0 & 0 & 0 & 0 & 0 & 0 & 0 \\ -\kappa\gamma & m_3 & -\phi_1 & 0 & 0 & 0 & 0 & 0 \\ -(1-\kappa)\gamma & 0 & m_4 & 0 & 0 & 0 & 0 & 0 \\ 0 & -\tau & -\eta & m_5 & 0 & 0 & 0 & 0 \\ -\epsilon & 0 & 0 & 0 & m_7 & 0 & 0 & 0 \\ 0 & -\epsilon & 0 & 0 & -\kappa\gamma & m_8 & -\phi_2 & 0 \\ 0 & 0 & -\epsilon & 0 & -(1-\kappa)\gamma & 0 & m_9 & 0 \\ 0 & 0 & 0 & -\epsilon & 0 & 0 & -\eta & -\tau + m_{10} \end{pmatrix}.$$

Hence, the control reproduction number of model (2), defined by $\mathcal{R}_e = \rho(FV^{-1})$ (where ρ is the spectral radius of the Next Generation Matrix FV^{-1}), is calculated as

$$\mathcal{R}_e = \frac{1}{2}\frac{\mu\gamma}{m_2 m_3 m_4 m_8 m_9 (m_1 m_7 - \theta\xi)^2}\left(\mathcal{R}_1 + \sqrt{\mathcal{R}_2}\right), \tag{11}$$

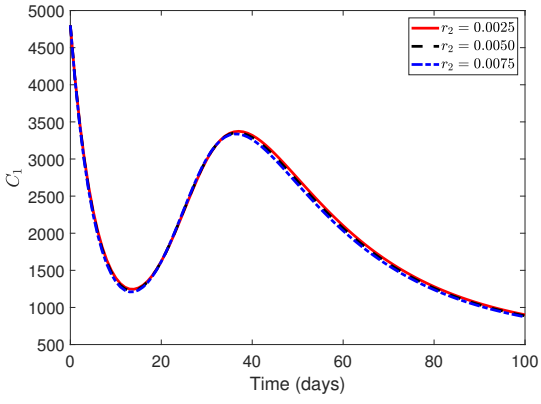

(a) Carrier in vaccine target susceptible population.

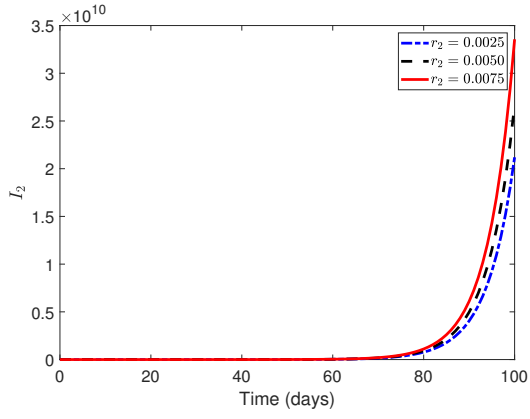

(b) Symptomatic infectious in non-vaccine target susceptible population.

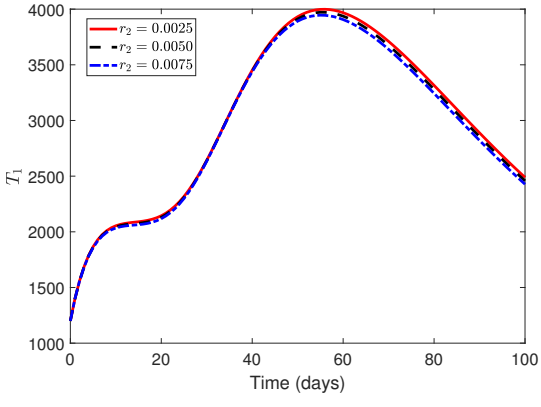

(c) Treated in vaccine target population.

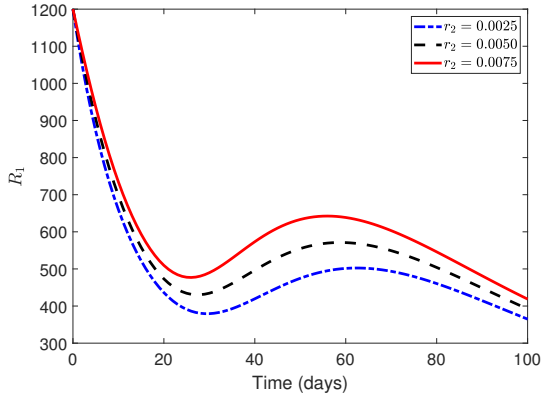

(d) Recovery due to treatment.

Figure 4. Simulation showing the dynamics of the states variables of model (2) with varying natural recovery of TB from carriers and symptomatic infectious.

where the expressions for $\mathcal{R}_1$ and $\mathcal{R}_2$ are provided in the Appendix.

4. NUMERICAL SIMULATIONS, RESULTS AND DISCUSSION

4.1. NUMERICAL SIMULATIONS

This part concentrates on the numerical simulations of the TB model (2). The entire simulations are carried out in MATLAB with *ode45* routine. Initial conditions are considered as follows: The total population at time $t = 0$ is taken as $N(0) = 1200000$, where 700000 are vaccine-target individuals and 500000 are non-vaccine-target population. We assumed that $I_1(0) = 2400$, $E_1(0) = 4 \times I_1(0)$, $C_1(0) = 2 \times I_1(0)$, $T_1(0) = 0.5 \times I_1(0)$, $R_1(0) = 0.5 \times I_1(0)$ and $V_1(0) = 3 \times I_1(0)$, so that $S_1(0) = 700000 - (E_1(0) + I_1(0) + C_1(0) + T_1(0) + R_1(0) + V_1(0))$. Also, we assume that $I_2(0) = 1200$, $E_2(0) = 4 \times I_2(0)$, $C_2(0) = 2 \times I_2(0)$, $T_2(0) = 0.5 \times I_2(0)$, $R_2(0) = 0.5 \times I_2(0)$, $V_2(0) = 3 \times I_2(0)$, so that $S_2(0) = 500000 - (E_2(0) + I_2(0) + C_2(0) + T_2(0) + R_2(0) + V_2(0))$. The model parameter values are displayed in Table 3. These values are chosen so that, using equation (11), the estimated value of $\mathcal{R}_e$ is approximately $\mathcal{R}_e = 2.596$. This represents the reality of settings (such as region or country) where TB is endemic.

4.2. RESULTS AND DISCUSSION

Figure 1 depicts the dynamic of varying effective transmission rate (β_1) of TB from carriers and symptomatic infectious individuals on vaccine target susceptible populations as shown in Figures 1a-1d. Figures 1a, 1b and 1c show a significant rise in the population of carrier, symptomatic infectious and treated in vaccine target population as the effective transmission rate (β_1) increases the carrier (C_1), symptomatic infectious (I_1) and treated population (T_1) increases and decreases as the effective transmission rate drops which shows a direct proportional relationship exist between β_1 and the the carrier (C_1), symptomatic infectious (I_1) and treated (T_1) individuals though very significant in vaccine target individuals as seen in Figures 1a, 1b and 1c while the decrease/increase was not drastic in Figure 1d. The implication is that any measure that will ensure the effective transmission rate is reduced should be implemented. Since it positively impacts the disease. These measures could include increased vaccination coverage, improved hygiene practices, and early detection and treatment of cases, as they all positively impact the disease.

Similarly, Figure 2 reveals the effect of varying effective transmission rates in the non-vaccine target population as seen in Figures 2a-2d. The clarity of these Figures, 2a, 2b and 2c, is evident in how they indicate a rise in the effective transmission rate results in a corresponding surge in the carrier, symptomatic infectious and the treated individuals in the non-vaccine target population. A rise or fall in the effective transmission rate does not result in the airline, symptomatic infectious and treated individuals in the vaccine target population.

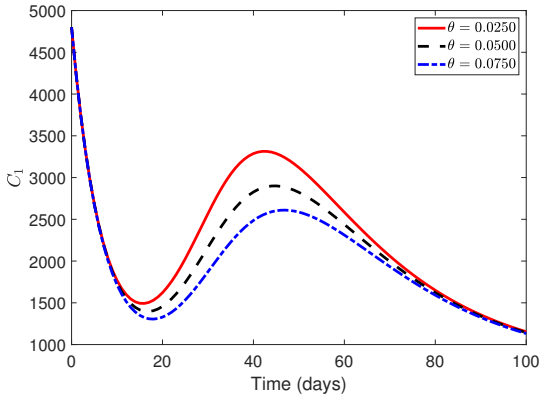

(a) Susceptible human.

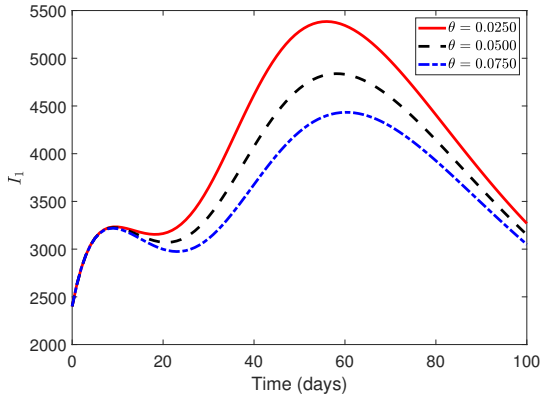

(b) Symptomatic infectious in non-vaccine target population.

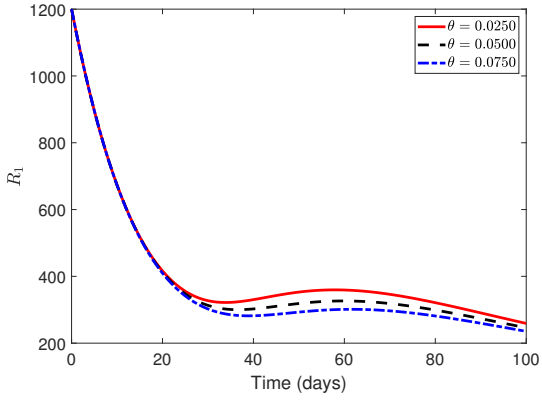

(c) Recovery due to treatment.

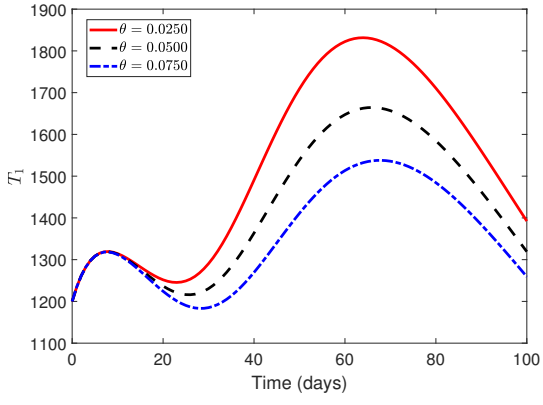

(d) treated in vaccine target susceptible population.

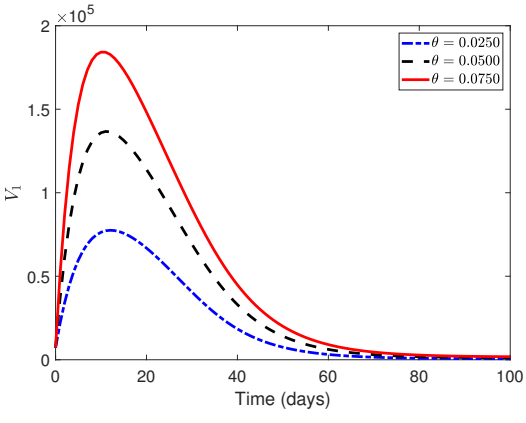

(e) Vaccinated in vaccine target population.

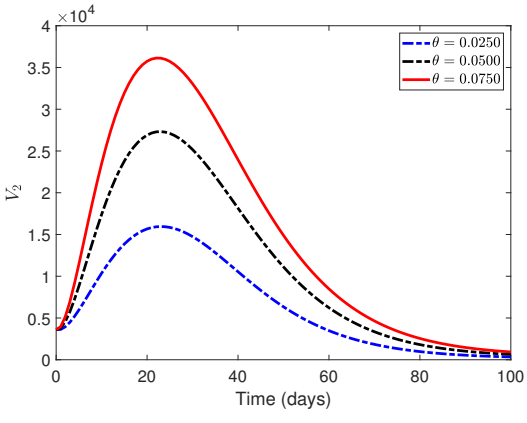

(f) Vaccinated in non-vaccine target population.

Figure 5. Simulation showing the dynamics of the states variables of model (2) with varying vaccine rate.

The significant increase in recovery of treated individuals in the vaccine target population is a promising finding, as depicted in Figures 3a and 3c. A 50% increase in the recovery rate leads to a corresponding 50% increase from the baseline values, while a 50% drop results in an equivalent decrease. Similarly, Figure 3b shows a direct proportional relationship. Although recovery due to treatment in the non-vaccine target carrier population was almost zero until around 80 days of the simulation, it witnessed a significant rise that continued and peaked at nearly 100 days of the simulation. Recovery of treated individuals in the vaccine target population saw a significant increase from the beginning of the simulation, which peaked at 40 to 70 days before falling slightly. This finding underscores the potential impact of vaccination in the target population on the recovery of treated TB-infected individuals.

It equally shows that the rise/decline in the recovery due to treatment was not significant in the treated non-vaccine target individuals, as shown in Figure 3d.

Figure 4 depicts the effect of varying natural recovery of TB in carrier, symptomatic infectious, treated, and recovered individuals from TB infection.

Initially, approximately 4,800 individuals naturally recovered

from TB as shown in Figure 4a. This was followed by a significant drop around the 10th-15th day of the simulation, with only about 1000 recovering on the 19th day. However, a subsequent rise occurred, and by the 30-40 days of the simulation, 3200 persons had recovered. A notable fall was observed on the 45th day, which persisted throughout the simulation. By the 100th day, less than 1000 people had recovered. The implication of these findings is that an increase in the immunity of the carrier vaccine target population could lead to a substantial increase in the number of individuals recovering naturally from TB infections, offering hope for the future of TB treatment.

Figure 4b illustrates that there was no recovery from TB infection in the initial 80 days of the simulation, even with fluctuations in the natural recovery rate from the baseline value. However, from the 80-100 days of the simulation, there was a noticeable rise in recovery, which increased or decreased as the natural recovery rate rose or fell from the baseline value. This suggests that even in the later stages of the simulation, there is potential for recovery, providing encouragement and motivation for further research and treatment development. Figure 4c highlights a significant rise in the number of individuals recovering from TB infection. The number increased from 1,200 on the first day to about 4,000 on the 45th day, peaking at 60 days. This peak suggests that the 60-day mark could be an optimal time for treatment. After this peak, there was a gradual decline in recovery rates, with 2,500 individuals recovering naturally from the disease by the 100th day. Figure 4d indicates a significant fall from a peak of 1200 at the initial stage of the simulation, which continues till 20 days, and on the 30th day, a slight rise followed by a fall maintained till the end of the simulation. The figure shows that the higher the natural recovery rate, the higher the number of individuals who recovered due to treatment.

Figure 5 shows that the higher the vaccination rate, the lower the population of TB carriers, the symptomatic infectious, the treated, the vaccinated in vaccine target and non-vaccine target populations.

5. CONCLUSION

Using an age-structured deterministic model that governs the transmission dynamics and control of tuberculosis (TB) in the presence of vaccination integrated into the eligible population, the mathematical model presented in this study examines the dynamics of TB. Using the next-generation matrix approach, the control reproduction number, $\mathcal{R}_e$, was calculated, which provided a numerical indication of the potential for TB transmission in the age-structured population; the qualitative analysis focuses on the disease-free equilibrium point and the model control reproduction number. The sensitivity analysis of the model highlights the most sensitive parameters for TB spread in the population. Furthermore, numerical analysis provides some useful information regarding the ways in which the vaccination rate and other important sensitive parameters affect the dynamics of TB transmission and control in an age-structured population. It is important to mention that constant vaccination rate is incorporated to the model analysed in this paper. Therefore, it is worth exploring the model of TB dynamics incorporating time-dependent vaccination by extending the model to an optimal control problem in a future study.

DATA AVAILABILITY

All data generated or analysed during this study are included in this article.

References

[1] M. Ronoh, R. Jaroudi, P. Fotso, V. Kamdoum, N. Matendechere, J. Wairimu, R. Auma & J. Lugoye, "A mathematical model of tuberculosis with drug resistance effects", Applied Mathematics **7** (2016) 1303. http://dx.doi.org/10.4236/am.2016.712115.

[2] World Health Organization, "Key facts on tuberculosis", 2024. [Online]. Accessed 06 January 2025. https://www.who.int/news-room/fact-sheets/detail/tuberculosis.

[3] World Health Organization, "Article on the overview, symptoms, treatment of tuberculosis", 2025. [Online]. Accessed 06 January 2025. https://www.who.int/health-topics/tuberculosis#tab=tab_1.

[4] E. Ibargüen-Mondragón, L. Esteva & E. M. Burbano-Rosero, "Mathematical model for the growth of Mycobacterium tuberculosis in the granuloma", Mathematical Biosciences & Engineering **15** (2018) 407. https://doi.org/10.3934/mbe.2018018.

[5] A. Abidemi, N. A. B. Aziz & E. Pindza, "Deterministic modelling of optimal control strategies for dengue fever transmission in two interconnected patches", Mathematical Sciences **18** (2024) 571. https://doi.org/10.1007/s40096-023-00517-0.

[6] S. Olaniyi, S. F. Abimbade, F. M. Chuma, O. A. Adepoju & O. D. Falowo, "A fractional-order tuberculosis model with efficient and cost-effective optimal control interventions", Decision Analytics Journal **8** (2023) 100324. https://doi.org/10.1016/j.dajour.2023.100324.

[7] F.O.Lawal, T.T. Yusuf, A. Abidemi & O. Olotu, "A non-linear mathematical model for typhoid fever transmission dynamics with medically hygienic compartment", Modeling Earth Systems and Environment **10** (2024) 6213. https://doi.org/10.1007/s40808-024-02111-2.

[8] B. Bolaji, A. Ibrahim, F. Ani, B. Omede & G. Acheneje, "A model for the control of transmission dynamics of human monkeypox disease in subsaharan africa", Journal of the Nigerian Society of Physical Sciences **6** (2024) 1800. https://doi.org/10.46481/jnsps.2024.1800.

[9] S. Ajao, I. Olopade, T. Akinwumi, S. Adewale & A. Adesanya, "Understanding the transmission dynamics and control of hiv infection: A mathematical model approach", Journal of the Nigerian Society of Physical Sciences **5** (2023) 1389. https://doi.org/10.46481/jnsps.2023.1389.

[10] E .C. Duru, G. C. E. Mbah, M. C. Anyanwu & N. T. Nnamani, "Modelling the co-infection of malaria and zika virus disease", Journal of the Nigerian Society of Physical Sciences **6** (2024) 1938. https://doi.org/10.46481/jnsps.2024.1938.

[11] K. A. Tijani, C. E. Madubueze & R. I. Gweryina, "Typhoid fever dynamical model with cost-effective optimalcontrol", Journal of the Nigerian Society of Physical Sciences **5** (2023) 1579. https://doi.org/10.46481/jnsps.2023.1579.

[12] A. B. Hogan, K. Glass, H.C. Moore & R. S. Anderssen, "Age structures in mathematical models for infectious diseases, with a case study of respiratory syncytial virus", in *Applications + Practical Conceptualization + Mathematics = fruitful Innovation. Mathematics for Industry* R. Anderssen (Ed.) **11** (2016) 105. https://doi.org/10.1007/978-4-431-55342-7_9.

[13] O. J. Peter, A. Abidemi, F. Fatmawati, M. M.Ojo & F. A. Oguntolu", Optimizing tuberculosis control: a comprehensive simulation of integrated interventions using a mathematical model" Mathematical Modelling and Numerical Simulation with Applications **4** (2024) 238. https://doi.org/10.53391/mmnsa.1461011.

[14] A. O. Sangotola, S. B. Adeyemo, O. A. Nuga, A. E. Adeniji & A. J. Adigun, "A tuberculosis model with three infected classes", Journal of the Nigerian Society of Physical Sciences **6** (2024) 1881. https://doi.org/10.46481/jnsps.2024.1881.

[15] E. D. Moya, A. Pietrus & S. M. Oliva, "A mathematical model for the study of effectiveness in therapy in tuberculosis taking into account associated diseases", Contemporary Mathematics **2** (2021) 77. https://ojs.wiserpub.com/index.php/CM/article/view/694.

[16] R. F. Appiah, Z. Jin, J. Yang & J .K. K. Asamoah, "Optimal control and cost-effectiveness analysis for a tuberculosis vaccination model with two latent classes", Modeling Earth Systems and Environment **10** (2024) 6761. https://doi.org/10.1007/s40808-024-02128-7.

[17] J. M. Trauer, J. T Denholm & E. S. McBryde, "Construction of a mathematical model for tuberculosis transmission in highly endemic regions of the Asia-Pacific", Journal of theoretical biology **358** (2014) 74. https:

//doi.org/10.1016/j.jtbi.2014.05.023.

[18] O. F. Lawal, T. T. Yusuf & A. Abidemi, ‘‘Modelling the impact of vaccination on transmission dynamics of Typhoid fever’’, Results in Control and Optimization **8** (2023) 100310. https://doi.org/10.1016/j.rico.2023.100310.

[19] P. van den Driessche & J. Watmough, ‘‘Reproduction numbers and subthreshold endemic equilibria for compartmental models of disease transmission’’, Mathematical biosciences **180** (2002) 29. https://doi.org/10.1016/S0025-5564(02)00108-6.